Cortisone-reductase deficiency associated with heterozygous mutations in 11β-hydroxysteroid dehydrogenase type 1

Alexander J. Lawson[a], Elizabeth A. Walker[b], Gareth G. Lavery[b], Iwona J. Bujalska[b], Beverly Hughes[b], Wiebke Arlt[b], Paul M. Stewart[b,1,2], and Jonathan P. Ride[a,1]

[a]School of Biosciences and [b]Centre for Endocrinology, Diabetes and Metabolism, School of Clinical and Experimental Medicine, University of Birmingham, Birmingham B15 2TT, United Kingdom

Edited by David W. Russell, University of Texas Southwestern Medical Center, Dallas, TX, and approved January 20, 2011 (received for review October 18, 2010)

In peripheral target tissues, levels of active glucocorticoid hormones are controlled by 11β-hydroxysteroid dehydrogenase type 1 (11β-HSD1), a dimeric enzyme that catalyzes the reduction of cortisone to cortisol within the endoplasmic reticulum. Loss of this activity results in a disorder termed cortisone reductase deficiency (CRD), typified by increased cortisol clearance and androgen excess. To date, only mutations in *H6PD*, which encodes an enzyme supplying cofactor for the reaction, have been identified as the cause of disease. Here we examined the *HSD11B1* gene in two cases presenting with biochemical features indicative of a milder form of CRD in whom the *H6PD* gene was normal. Novel heterozygous mutations (R137C or K187N) were found in the coding sequence of *HSD11B1*. The R137C mutation disrupts salt bridges at the subunit interface of the 11β-HSD1 dimer, whereas K187N affects a key active site residue. On expression of the mutants in bacterial and mammalian cells, activity was either abolished (K187N) or greatly reduced (R137C). Expression of either mutant in a bacterial system greatly reduced the yield of soluble protein, suggesting that both mutations interfere with subunit folding or dimer assembly. Simultaneous expression of mutant and WT 11β-HSD1 in bacterial or mammalian cells, to simulate the heterozygous condition, indicated a marked suppressive effect of the mutants on both the yield and activity of 11β-HSD1 dimers. Thus, these heterozygous mutations in the *HSD11B1* gene have a dominant negative effect on the formation of functional dimers and explain the genetic cause of CRD in these patients.

The interconversion of inactive glucocorticoids (cortisone in man and 11-dehydrocorticosterone in rodents) and hormonally active glucocorticoids (cortisol and corticosterone) is catalyzed by 11β-hydroxysteroid dehydrogenase type 1 (11β-HSD1), an ER-localized membrane-bound enzyme (1). 11β-HSD1 is a member of the short-chain dehydrogenase reductase (SDR) superfamily of enzymes and naturally exists as a homodimer (2–5), although some studies have suggested that it also may function as a homotetramer (6). Unusually for an SDR enzyme, 11β-HSD1 has an N-terminal membrane anchor (7, 8), with a small portion of the N-terminal segment of the enzyme present in the cytosol. The glycosylated catalytic C-terminal domain exists in the lumen of the endoplasmic reticulum (8) and putatively dips into the membrane lipid bilayer to facilitate access to steroid substrates (4, 5). The reaction direction that 11β-HSD1 catalyzes is determined by the relative abundance of $NADP^+$ and NADPH (9, 10). When purified, 11β-HSD1 acts more readily as a dehydrogenase, inactivating cortisol to cortisone; however, in the presence of a high NADPH/$NADP^+$ ratio, generated in vivo through the activity of microsomal hexose-6-phosphate dehydrogenase (H6PDH) (11), 11β-HSD1 switches to ketoreductase, with the generation of active glucocorticoid in key target tissues of glucocorticoid action, such as liver and adipose. In these tissues, 11β-HSD1 ketoreductase activity has been shown to enhance hepatic glucose output (12) and adipogenesis (13), respectively.

Cortisone reductase deficiency (CRD) is a disorder in which there is a failure to regenerate the active glucocorticoid cortisol (F) from cortisone (E) via 11β-HSD1 (1). A lack of cortisol regeneration stimulates ACTH-mediated adrenal hyperandrogenism, with males manifesting in childhood with precocious pseudopuberty and females presenting in adolescence and early adulthood with hirsutism, oligoamenorrhea, and infertility. Biochemically, CRD has been diagnosed through the assessment of urinary cortisol and cortisone metabolites, such as measuring the ratio of tetrahydrocortisol (THF) plus 5α-THF to tetrahydrocortisone (THE) and the ratio of cortols to cortolones (Fig. 1*A*). In CRD patients, the THF + 5α-THF/THE ratio is typically <0.1 (reference range, 0.7–1.2) (1).

CRD was first described more than 20 years ago (14). To date, 11 individuals have been reported (14–19), and the *HSD11B1* gene has been analyzed in seven CRD kindreds. Although no functional mutations were found in the coding regions of the *HSD11B1* gene, the analysis revealed an A insertion and a T-G substitution in intron 3 in some patients. This 83557A/83597T-G haplotype was associated with a 28-fold reduction in 11β-HSD1 mRNA in adipose tissue with complete loss of ketoreductase activity, indicating a potential biomarker for CRD. However, due to the heterozygous presence of this locus in 25% of normal individuals and homozygous presence in 3%, these mutations cannot account for the CRD phenotype. Based on the critical need of 11β-HSD1 for NADPH, we focused our attention on H6PDH, a G6PDH-like enzyme responsible for NADPH generation within the endoplasmic reticulum. We reported four novel homozygous mutations in the *H6PD* gene in four individuals with florid CRD (THF+5α-THF/THE ratio ≤0.05). None of these patients had mutations in the *HSD11B1* gene (20), and accordingly, the term "apparent" cortisone reductase deficiency (ACRD) was applied. Each mutation abolished H6PDH activity and resulted in a lack of NADPH cofactor to support the ketoreductase activity of 11β-HSD1 (20).

Here we report the first examples of heterozygous mutations in the coding sequence of the *HSD11B1* gene in two patients presenting with hyperandrogenism and premature pseudopuberty with biochemical features indicative of CRD, in whom the *H6PD* gene was normal. Using both bacterial and mammalian cell expression systems, we investigated the effect of the mutations expressed either alone or together with WT 11β-HSD1.

Author contributions: A.J.L., E.A.W., P.M.S., and J.P.R. designed research; A.J.L., E.A.W., G.G.L., I.J.B., B.H., and J.P.R. performed research; A.J.L., E.A.W., G.G.L., W.A., P.M.S., and J.P.R. analyzed data; and A.J.L., E.A.W., P.M.S., and J.P.R. wrote the paper.

The authors declare no conflict of interest.

This article is a PNAS Direct Submission.

[1]P.M.S. and J.P.R. contributed equally to this work.

[2]To whom correspondence should be addressed. E-mail: p.m.stewart@bham.ac.uk.

This article contains supporting information online at www.pnas.org/lookup/suppl/doi:10.1073/pnas.1014934108/-/DCSupplemental.

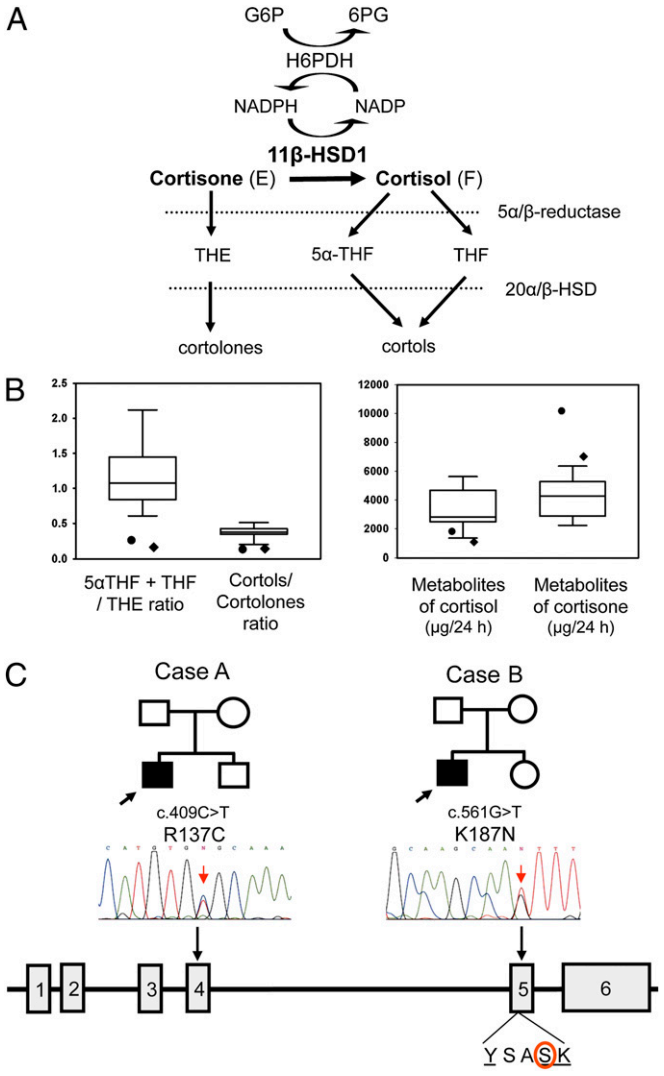

Fig. 1. Urinary steroid analysis and molecular genetic assessments of cases A and B. (*A*) Schematic representation of the interaction between 11β-HSD1 and H6PDH. H6PDH generates NADPH, enabling 11β-HSD1 ketoreductase activity to convert cortisone (E) to cortisol (F). Cortisone and cortisol are metabolized by 5α reductases to produce THE and 5β reductases to produce 5α-THF and THF. The 20α- and 20β-HSDs further metabolize these to cortolones and cortols. These metabolites are detectable in urine and serve as biomarkers of 11β-HSD1 activity. (*B*) Urinary cortisol and cortisone metabolite levels/ratios for case A (●) and case B (♦). Normal ranges for urinary steroid analysis are depicted as box-and-whisker plots and were determined using sex and age specific normal cohorts, which for the purposes of this report are drawn from a cohort of males age 10–16 y. (*C*) *HSD11B1* gene mutations in CRD cases A and B. Pedigrees for each case are shown with the affected male being the filled square. The gene structure for *HSD11B1* is shown as filled boxes for exons and intervening lines for introns. A sequencing trace is shown indicating the affected nucleotide. The position and alteration at the nucleotide and protein levels are given above each trace. The position of the K187N missense mutation relative to the highly conserved YxxxK catalytic motif is shown below the gene schematic.

This study included developing a bacterial system that facilitates the purification of recombinant heterodimers (mutant/WT).

Results

Urinary Steroid Metabolite Analysis. Results for the two index cases, A and B, are presented in Table 1 and Fig. 1*B*. Measurement of urinary cortisone and cortisol metabolites revealed abnormally low THF+5αTHF/THE ratios, 0.26 in case A and 0.16 in case B, both lower than age- and sex-specific reference cohorts. The ratio of cortols to cortolones, which also reflects the secondary metabolism of cortisol and cortisone, was also low compared with age- and sex-specific reference cohorts (Fig. 1*B*). In addition, measurement of absolute levels of cortisol and cortisone metabolites revealed low to normal levels of cortisol metabolites but very high levels of cortisone metabolites compared with age- and sex-specific reference cohorts (Fig. 1*B*), again in keeping with a blockage in 11β-HSD1–mediated cortisone-to-cortisol conversion. We extended this analysis to the parents of cases A and B and found a maternal inheritance of the biochemical phenotype. The mothers had urine biochemistry identical to that found in their offspring, with lower THF+5α-THF/THE and cortol/cortolone ratios, whereas both fathers demonstrated normal values for these parameters (Table 1). To examine secondary activation of the hypothalamic-pituitary-adrenal axis, we summed the values of all cortisol and cortisone metabolites to provide an index of total secretion rate (reported as μg/24 h) (21). An increased cortisol secretion rate was clearly suggested in both patients and their mothers, but levels for the fathers were within the reference range (Table 1).

Cases A and B exhibited higher levels of excreted androsterone, etiocholanolone, and dehydroepiandrosterone (DHEA). The cumulative excretion of androsterone + etiocholanolone + DHEA reflects the degree of adrenal androgen output, which was 4,945 μg/24 h (sex- and age- adjusted reference range, 352–1,774) for case A and 7,740 μg/24 h (sex- and age- adjusted reference range, 2,960–4,880) for case B. Similarly, the mothers of cases A and B showed androgen metabolite excretion levels either at the upper range of normal (mother of case A, 5,579 μg/24 h) or higher (mother of case B, 8,248 μg/24 h) (reference range, 1,152–5,828). In contrast, androgen excretion in the fathers of cases A and B were normal at 5,639 μg/24 h and 6,354 μg/24 h, respectively (reference range, 2,650–7,863) (Table 1).

Molecular Analysis of *H6PD* and *HSD11B1* Genes. No mutations were identified in *H6PD*. However, sequencing of *HSD11B1* revealed two sequence variants in cases A and B, one each in the heterozygous state, which were not detected in 120 control chromosomes. Case A was heterozygous for a maternally inherited c.409C > T mutation in exon 4 generating an arginine-to-cysteine missense mutation (R137C) (Fig. 1*C*). Case B was heterozygous for a maternally inherited c.561G > T mutation in exon 5 generating a lysine-to-asparagine missense mutation (K187N) (Fig. 1*C*).

Functional Analysis of *HSD11B1* Mutations. Sequence alignments indicate that Arg^{137} and Lys^{187} are strictly conserved within 11β-HSD1 proteins from different species (Fig. 2 *A* and *B*). Examination of the position of Arg^{137} in crystal structures of 11β-HSD1 (Protein Data Bank entries 2BEL, 2IRW, 3FCO, 1XU7, and 1XU9) reveals a potentially vital role in dimerization of the enzyme. Arg^{137} on helix αE of the A subunit is positioned at the edge of the dimer interface and forms a salt bridge with the highly conserved residue Glu^{141} on the B subunit (Fig. 2 *C* and *D*). A corresponding interaction between Arg^{137} on the B subunit and Glu^{141} on the A subunit forms a second bridge.

Expression of 11β-HSD1 Homodimers in Mammalian Cells. To further address the functional consequence of these mutations, the R137C and K187N mutants were stably expressed in vitro in HEK 293 cells, and 11β-HSD1 enzyme activity was measured by the conversion of cortisone to cortisol within the intact cells. HEK 293 cells mock-transfected with empty vector had no detectable activity (Fig. 3*A*). Upon transfection with WT 11β-HSD1, robust activity was seen; however, transfection of cells to similar levels (as evidenced by similar mRNA expression; Fig. 3*B*) with the two mutant 11β-HSD1 constructs produced only ~5% of WT activity from the R137C mutant and no activity from the K187N mutant (Fig. 3*A*). Western blot analyses of total cell lysates indicated that compared with WT, low levels of 11β-HSD1 protein accumulated from the R137C mutant (Fig. 3*C*), whereas the K187N construct

Table 1. Diagnostic ratios and summation of urinary cortisol and androgen metabolites as assessed by GC/MS in patients and their family members

	(THF+5α-THF)/THE	Cortols/cortolones	Total androgens, μg/24 h	Total cortisol metabolites, μg/24 h
Case A (46,XY)	0.26*	0.13*	4,945†	10,770†
Mother A	0.29*	0.13*	5,579	12,701†
Father A	0.95	0.61	5,639	9,211
Case B (46,XY)	0.16*	0.14*	7,740†	8,151
Mother B	0.50*	0.17*	8,248†	15,073†
Father B	0.75	0.33	6,354	11,319

Total metabolites reflect 24-h secretion rates of adrenal cortisol and androgens, respectively. Total androgens represent androsterone + etiocholanolone + dehydroepiandrosterone. Total cortisol metabolites represent THF + 5α-THF + THE + cortols + cortolones + free F + free E.

*Decreased below the minimum of the sex- and age-specific reference cohort.

†Increased above the maximum of the sex- and age-specific reference cohort.

was capable of producing some 11β-HSD1 protein, although the K187 protein was clearly inactive.

Bacterial expression systems were then used to fully characterize the effect of these mutations on kinetic parameters of the enzyme and also to investigate their possible effects when produced as WT/mutant heterodimers, as would be found in vivo in cases A and B. The expression system used entailed the expression of an N-terminally truncated version of 11β-HSD1 (i.e., minus the transmembrane anchor), which contained an additional mutation (F278E) designed to promote solubility and monodispersity of the protein without affecting enzyme activity (22).

Analysis of 11β-HSD1 Homodimers Expressed in Bacteria. Expression of WT homodimeric 11β-HSD1 protein from either the pRSF-1 (His-tag) or pET-51 (Strep-tag) vector in *Escherichia coli* yielded similar amounts of purified soluble protein with similar k_{cat} and K_m values to those reported previously (22) for a pET-28 (His-tag) construct (Fig. 4). However, the introduction of the K187N mutant into pRSF-1 resulted in a complete absence of any soluble protein, whereas the equivalent R137C construct yielded 6-times less soluble protein than WT (Fig. 4*A*). The yield of total protein (soluble + insoluble) from these types of vectors is not significantly affected by the mutations (22). Thus, both mutations drastically affected either subunit folding or dimer assembly/stability in this expression system. The purified homodimeric R137C mutant protein also showed a small decrease in turnover rate (k_{cat}), but with no significant change in K_m (Fig. 4 *B* and *C*). This is in agreement with findings of a previous preliminary study using pET-28 constructs (22) and parallels the results obtained from the mammalian expression system (Fig. 3).

Analysis of 11β-HSD1 Heterodimers. To fully investigate the effects of the R137C and K187N mutations on heterodimer formation and activity, bacterial cells were simultaneously transformed with both the pRSF-1 and the pET-51 plasmids, with one vector containing WT 11β-HSD1 and one vector containing either the R137C mutant or the K187N mutant. The effect of this dual expression of WT and mutant constructs was initially estimated by assaying total enzyme activity and relative amounts of His/Strep tag in cleared lysates of the bacterial cells (Fig. 5). When both plasmids contained WT protein, the pET-51 plasmid expressed more soluble protein than the pRSF-1 plasmid (Fig. 5*B*). This could be due to either greater promoter efficiency or a higher copy number of pET-51. When the R137C or K187N mutations were present in the pRSF-1 plasmid, a 40–50% decrease in total enzyme activity was observed (Fig. 5*A*). There was also a significant reduction (by 55–65%) in the amount of mutant polypeptide found in the soluble fraction, although the level of soluble WT subunit (from pET-51) was much less affected (Fig. 5*B*). A greater decrease in enzyme activity (of 85–95%) was observed in the reverse situation, when the mutants were present in the pET-51 plasmid with pRSF-1 expressing WT protein (Fig. 5*A*). This was accompanied by substantial decreases in the amounts of both WT and mutant polypeptide in the soluble fraction (Fig. 5*B*). This suggests that in this situation, because of the greater mutant protein production by the pET-51 plasmid, more WT monomers were interacting with mutant monomers and forming unstable/insoluble heterodimers or other complexes, resulting in the reduced enzyme activity. To confirm that the effects seen were not due to anomalies of the chosen bacterial expression system or the tags, full-length untagged mutant

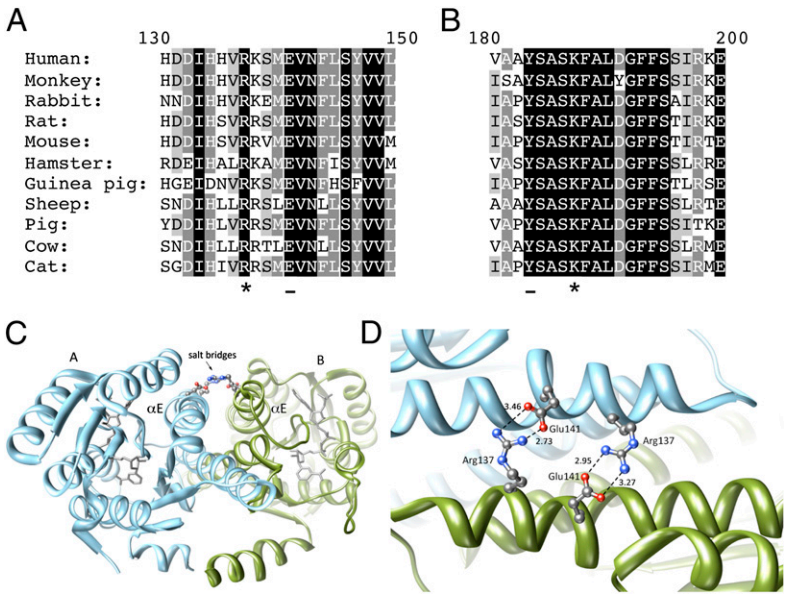

Fig. 2. The structural importance of the 11β-HSD1 mutations R137C and K187N. (*A*) Alignment showing the strict conservation of Arg^{137} (marked with *) in 11β-HSD1 protein sequences from different species. Arg^{137} interacts to form a salt bridge with conserved residue Glu^{141} (underlined on the alignment) on the opposing subunit. (*B*) Alignment showing the conservation of Lys^{187} (marked with *) across species. Lys^{187} forms part of the catalytic tetrad, which includes the adjacent residue Tyr^{183} (underlined in the alignment). (*C*) A ribbons representation of the crystal structure of the 11β-HSD1 dimer (Protein Data Bank code: 2bel, chains A and B) showing the salt bridges between Arg^{137} and Glu^{141} on the αE helices of opposing subunits. Arg^{137} and Glu^{141} are represented in ball-stick format colored by heteroatom. (*D*) A closer view of the side-chain interactions between the two pairs of Arg^{137} and Glu^{141} residues at the subunit interface of 11β-HSD1 (Protein Data Bank code: 2bel, chains A and B), showing the close interaction (<4Å) between the heavy atoms. The salt bridges are of the fork-fork class (35) in this structure, although other 11β-HSD1 crystal structures are of the fork-stick type. These interactions may promote correct orientation of the subunits during dimer formation, as well as stabilize the final assembly. Structural images were produced using UCSF Chimera from the University of California San Francisco's Resource for Biocomputing, Visualization, and Informatics (supported by National Institutes of Health Grant P41 RR-01081) (36). Distances calculated between nitrogen and oxygen atoms are shown in Å.

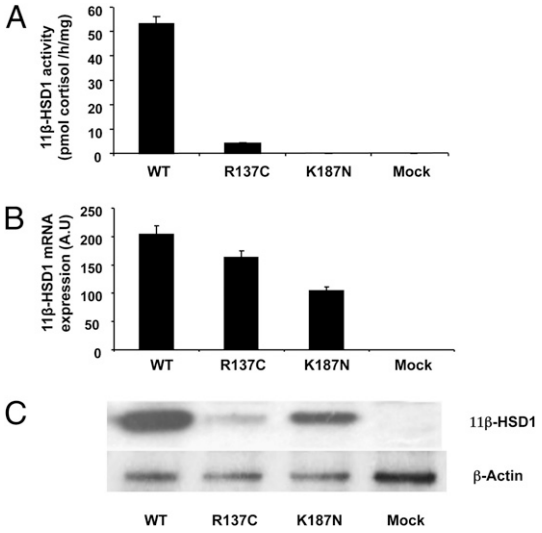

Fig. 3. 11β-HSD1 ketoreductase activity, mRNA levels, and protein expression from homodimers expressed in stably transfected HEK293 cells. (*A*) 11β-HSD1 enzyme activity assays in HEK 293 cells mock-transfected or stably transfected with the WT and mutant cDNA constructs expressed as pmol cortisol produced/mg of protein/h (mean ± SEM; $n = 3$). Mock-transfected cells exhibited no 11β-HSD1 ketoreductase activity. Activity was 53.1 ± 3.1 in cells transfected with WT 11β-HSD1 and 4.1 ± 0.4 for the R137C mutant. No ketoreductase activity was detectable for the K187N mutant. (*B*) Real-time PCR assessment of *HSD11B1* gene expression in stably transfected clones compared with mock-transfected controls, indicating overexpression of *HSD11B1* mRNA in transfected lines, expressed in arbitrary units (AU). (*C*) Western blot analysis of whole cell extracts from HEK293-transfected cells. High levels of WT protein were produced with significantly lower levels from the R137C and K187N mutants.

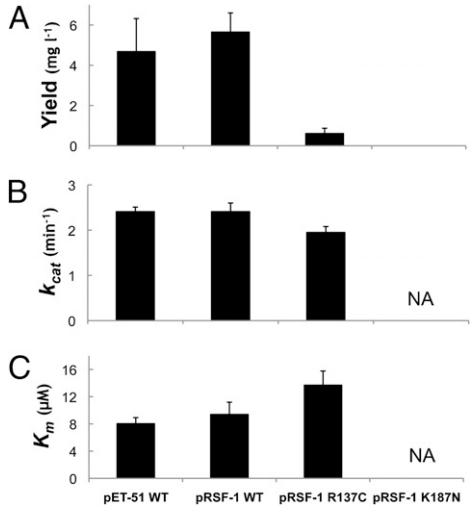

Fig. 4. Yield of soluble protein and kinetic parameters of homodimers of 11β-HSD1 in the bacterial expression system. (*A*) Yield of soluble, purified 11β-HSD1 protein. Values are given in mg of protein purified per L of LB broth. Bars represent SEM ($n = 3$). (*B*) Turnover rates (k_{cat}) for the conversion of cortisol to cortisone. The decrease observed for the R137C mutant is statistically significant ($P < 0.05$, ANOVA). No data are available for the K187N mutant, because no soluble protein was produced. (C) K_m values for cortisol for WT and mutant proteins. The increase observed for the R137C mutant compared with WT is not statistically significant. No data are presented for the K187N mutant, because no soluble protein was produced. Bars represent SEM ($n = 3$).

and WT sequences were coexpressed in mammalian (HEK293) cells using a bicistronic vector. Lysates of stably transfected cells reproducibly demonstrated a dramatic reduction in 11β-HSD1 activity when either of the mutants was coexpressed with the WT sequence (Fig S1*A*). A reduction in total 11β-HSD1 protein in the cleared lysates was also observed when the mutants were included (Fig S1*C*), although the reduction with K187N was less dramatic than that with R137C.

To elucidate the true effect of both the R137C and K187N mutants on heterodimer formation and activity, a protocol was developed to purify mutant/WT heterodimers from bacterial lysates. This procedure exploited the different N-terminal tags on the different constructs and involved diluting the protein solutions heavily to ensure the presence of dimeric protein, but not tetrameric protein (22). After the procedure, the presence of true heterodimers was also confirmed by analysis of the relative proportions of His and Strep tags by standardized Western blot analyses. All purified preparations showed equal levels of the two tags (Fig. S2), as would be expected for true heterodimers. An analysis of heterodimer properties revealed that the WT-His/WT-Strep hybrid dimer control had unchanged k_{cat} and K_m values compared with the pET-51– and pRSF-1–derived WT homodimers (Table 2). The yield of soluble protein was not that high, which is not surprising given the number of chromatographic steps in the procedure. However, the WT/R137C hybrid dimer showed a pronounced reduction in yield (>80%) compared with the WT/WT hybrid dimer (Table 2), along with a slight reduction in k_{cat}. The WT/K187N hybrid dimer exhibited a similar large decrease in yield compared with WT/WT; however, the protein produced in that case was completely inactive (Table 2). Thus, including mutant strands in the expression system resulted in reduced levels of soluble WT 11β-HSD1, as well as reduced enzyme activity of the WT subunits when present in heterodimers.

Discussion

Before the present work, deficient reduction of cortisone to cortisol had been attributed only to mutations in the gene encoding H6PDH, the enzyme that supplies NADPH to 11β-HSD1 (20), a condition subsequently termed apparent cortisone reductase deficiency (ACRD). Individuals with an inactivating mutation in *H6PD* lose 11β-HSD1 ketoreductase activity but gain dehydrogenase activity, leading to a dramatically increased cortisol clearance rate and an extreme biochemical phenotype typified by very low THF+5αTHF/THE ratios. However, our findings suggest that mutations in the coding region of the *HSD11B1* gene itself also may be important in some cases, even when present in a heterozygous state. We examined the *HSD11B1* gene in two patients presenting with hyperandrogenism and premature pseudopuberty with biochemical features indicative of a milder form of CRD, in whom the *H6PD* gene was normal. Given these patients' milder defect in cortisol metabolism, we hypothesized that the underlying genetic cause in these cases might be inactivating mutations in *HSD11B1*. Such mutations would result in loss of both ketoreductase activity and dehydrogenase activity, as seen in 11β-HSD1 KO mice (12), manifesting as a less severe biochemical phenotype compared with *H6PD* mutations in man and H6PDH KO mice; indeed, in cases A and B, the urinary THF +5αTHF/THE ratio was ∼0.2, compared with the value of <0.05 seen in ACRD. Two novel mutations (R137C and K187N) in *HSD11B1* were identified in cases A and B. Although these two cases were heterozygous for the mutations rather than homozygous, it was possible that because of the dimeric nature of 11β-HSD1, the expression of mutant subunits could interfere in some way with the activity of the coexpressed WT subunits; that is, the mutations could have a dominant-negative character. We addressed this question using our previously developed bacterial expression system (22, 23), together with a mammalian cell expression system.

Sequence alignment indicated that both Arg^{137} and Lys^{187} are strictly conserved within 11β-HSD1 proteins from different species (Fig. 2 *A* and *B*). Lys^{187} is a component of the YxxxK motif that is strictly conserved within the SDR family, being part of the

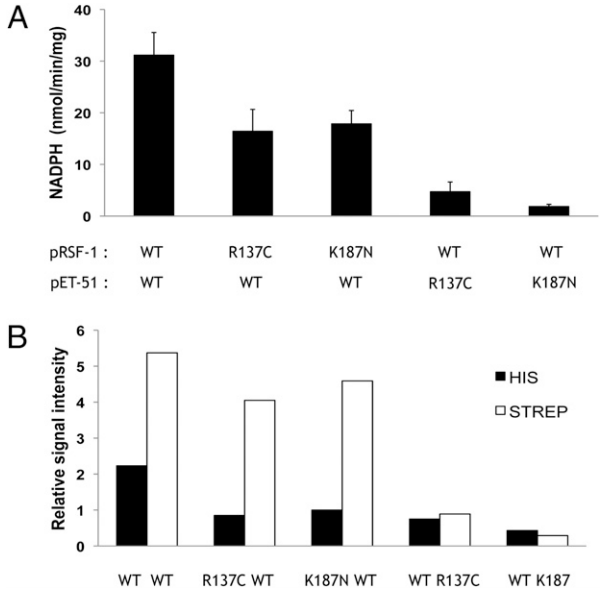

Fig. 5. Effect of coexpression of mutant and WT 11β-HSD1 constructs in *E. coli*. (*A*) Specific enzyme activity of cleared lysates of bacteria transformed with two plasmids: pET-51, encoding a Strep-tagged protein, and pRSF-1, encoding a His_6-tagged protein. Enzyme activity was measured in the dehydrogenase direction (conversion of cortisol to cortisone) at saturating substrate concentrations. Expression of the mutants from the pRSF1 plasmid resulted in a decrease in enzyme activity, but to a much lesser degree than when the mutants were in pET-51. Bars represent SEM (n = 3). (*B*) Western blot densitometry analysis of relative concentrations of His and Strep tags in cleared bacterial lysates. Expression of either mutant caused a reduction in both mutant and WT polypeptides found in soluble form, with a greater effect when the mutants were in pET-51. Note the greater expression of Strep-tagged protein driven by pET-51 compared with His-tagged protein from pRSF-1 in the WT/WT control.

core catalytic tetrad of Asn, Ser, Tyr, and Lys required for enzyme activity (24). In most of the SDR enzymes characterized to date, the highly conserved Tyr residue functions as general acid/base catalyst, whereas the Lys facilitates catalysis, acting as part of a proton relay and interacting with the nicotinamide cofactor. In a previous study, site-directed mutagenesis of this residue in rat 11β-HSD1 resulted in complete loss of enzyme activity (25). The present study confirms the importance of this residue to human 11β-HSD1 activity; no enzyme activity could be detected when the K187N mutant was expressed in either mammalian or bacterial cells. In the bacterial system, no soluble protein could be detected at all, indicating the probable additional importance of this residue to structural stability. Lys^{187} is known to ligate the 2- and 3-ribose hydroxyls of the nicotinamide cofactor in 11β-HSD1 (6), and cofactor binding may be essential for correct folding/stability. Inability to bind cofactor also would impair binding of the inhibitor carbenoxolone, which is added to the bacterial system to promote the expression of properly folded, soluble protein—hence probably explaining the even lower levels of soluble protein found in the bacterial system compared with the mammalian cell system.

Table 2. Yield of soluble protein and kinetic parameters and for the various hybrid dimers of 11β-HSD1 purified from the bacterial expression system

Construct				
pRSF-1 (His tag)	pET-51 (Strep tag)	Yield (mg l^{-1})	k_{cat} (min^{-1})	K_m (μM)
WT	WT	0.047 ± 0.003	2.29 ± 0.18	7.62 ± 1.52
R137C	WT	0.008 ± 0.001	1.73 ± 0.15	14.72 ± 2.81
K187N	WT	0.008 ± 0.004	—	—

The k_{cat} and K_m values for the WT-His/WT-Strep heterodimer construct are not significantly different from the previous homodimeric WT constructs, although the yield of the heterodimer is lower. Heterodimeric R137C/WT constructs have decreased k_{cat} values and increased K_m values. There also is a significant reduction in the yield of soluble protein compared with the WT/WT equivalent. Heterodimeric K187/WT constructs have no detectable enzyme activity, in addition to a significant reduction in the yield of soluble protein. Yield values are given in mg of protein per L of LB broth ± SEM (n = 3).

11β-HSD1 is a dimeric enzyme, and although a mutant K187N homodimer would be expected to be inactive, the effect of heterodimer formation between WT and mutant subunits (as could occur in heterozygous humans, such as case B) was uncertain. The two subunits of 11β-HSD1 are closely intertwined, facilitating a close structural interplay between the monomers (4, 5). Thus, the K187N mutation in one subunit possibly could negatively affect the activity of an adjacent WT subunit. This type of effect has been reported for the enzyme biotin carboxylase, where an inactivating mutation in the active site of one monomer of the protein was found to have a dominant negative effect on the other monomer, resulting in a 285-fold decrease in activity (21). The experimental evidence from the hybrid WT/K187N dimer constructed in the present study suggests that this is indeed the case for 11β-HSD1. The purified heterodimer had no detectable enzyme activity. However, the simultaneous expression of the K187N mutant had a second, unexpected effect on the coexpressed WT 11β-HSD1, substantially reducing the yield of soluble WT polypeptide. Therefore, it seems likely that the mutant subunit is capable of interacting with WT subunits to cause unstable and ultimately insoluble aggregates; that is, the mutation exerts a dominant negative effect on protein yield as well as activity.

Expression of the R137C mutation as a homodimer in either mammalian or bacterial cells also resulted in a dramatic decrease in the yield of functional soluble protein, coupled with a more minor effect on the k_{cat} of the purified enzyme. An explanation for this effect lies in the potentially vital role of Arg^{137} in dimerization of the 11β-HSD1 enzyme. This conserved residue forms two interfacial salt bridges with the similarly conserved Glu^{141} between each pair of subunits. Salt bridges, particularly those involving arginine, can play a prominent role in protein stability (26–28), including stabilizing intersubunit interactions (29) and guiding the subunits to the correct docked arrangement (30, 31). Of relevance here is that an Arg–Asp salt bridge at the dimeric interface of another SDR, 3α-hydroxysteroid dehydrogenase/carbonyl reductase, has recently been shown to be essential for conformational stability, oligomeric integrity, and enzymatic activity (32). Thus, salt bridges may be a common way in which dimer formation is promoted, and dimer integrity maintained, in the SDR family.

As with the K187N mutant, coexpression of the R137C mutant with WT 11β-HSD1 resulted in a marked suppression of soluble proteins, including WT strands. Interestingly, purifying the WT-R137C hybrid dimer from this system led to similar reductions in yield (~80%) and k_{cat} (~20%) to those seen when homodimeric R137C was compared with homodimeric WT (Fig. 3). This implies that the deleterious effects of the R137C mutation can extend across the dimer interface to influence activity of the other, nonmutant monomer.

In conclusion, we have shown that K187N and R137C have deleterious effects on 11β-HSD1 activity by compromising the production and stability of the dimeric protein, and thus true CRD due to mutations in *HSD11B1* may be a further monogenic cause of hyperandrogenism/premature pseudopuberty. There remains intense interest in the potential role of 11β-HSD1 inhibitors in treating facets of the metabolic syndrome, notably insulin resistance, glucose intolerance, and obesity (33). Our cases were young boys referred from outside our center, and to date we have not been able to perform metabolic phenotyping studies. Nonetheless, the two cases illustrate a potential pitfall of

selective 11β-HSD1 inhibition: adrenal hyperplasia and hyperandrogenism. Future clinical studies are needed to define the relevance of this finding in older subjects.

Materials and Methods

Further details regarding the materials and methods used are provided in *SI Materials and Methods*.

Cases. Approval for all studies was obtained from the local hospital Ethics Committees. Cases A and B were minors, and parental consent was obtained. Case A presented at age 8 y with features of premature pubarche and advanced bone age. Case B presented at age 13 y with recent onset obesity (body mass index, 32.5 kg/m^2), clinical signs suggestive of insulin resistance (acanthosis nigricans), and hyperandrogenemia.

Urinary Steroid Metabolite Analysis. Adrenal-derived urinary steroid metabolites were measured on complete 24-h collections by GC/MS-selected ion monitoring, as reported previously (17,34).

Functional Analysis: Mammalian Cell Expression of Homodimers and Heterodimers. Full-length homodimers were expressed from WT or mutant HSD11B1 cDNA contained in pCR3 (Invitrogen). In addition, WT and mutant HSD11B1 sequences were cloned into the pIRES vector (Clontech) to allow high level expression of both genes from the same bicistronic mRNA transcript. Mammalian HEK 293 cells were transfected with WT and/or mutant HSD11B1 constructs, and three cell lines were derived from three separate transfection experiments.

Bacterial Expression and Purification of Recombinant 11β-HSD1 Homodimers. All experiments used an N-terminally truncated version of 11β-HSD1 (i.e., minus the transmembrane anchor), which contains an additional mutation (F278E) designed to promote solubility and monodispersity of the protein without affecting enzyme activity (22). Constructs were expressed from pRSF-1b or pET-51b(+) vectors (Novagen) with either His or Strep tags. Enzymes were purified and activity was measured as described previously (22).

Bacterial Expression and Purification of 11β-HSD1 Heterodimers. To enable expression of WT and mutant 11β-HSD1 heterodimers, *E. coli* BL21(DE3) cells were cotransformed with pET-51b(+) and pRSF-1b containing the WT or mutant 11β-HSD1 constructs. Heterodimers were purified by repeated-affinity chromatography.

Measurement of 11β-HSD1 Activity. Dehydrogenase activity of bacterially expressed 11β-HSD1 was monitored by spectrofluorimetry.

ACKNOWLEDGMENTS. We thank Dr. Nandu Thalange for patient samples and clinical data on case A, Dr. Jerry K. Wales for samples relating to case B, and Susan V. Hughes for technical support. This work was supported by a Medical Research Council studentship (to A.J.L.), Wellcome Trust Programme Grant 066357 and Project Grant 074088 (to E.A.W. and P.M.S.), and Medical Research Council Programme Grant G0900567 (to W.A.).

1. Tomlinson JW, et al. (2004) 11beta-hydroxysteroid dehydrogenase type 1: A tissue-specific regulator of glucocorticoid response. *Endocr Rev* 25:831–866.
2. Maser E, Wsol V, Martin HJ (2006) 11Beta-hydroxysteroid dehydrogenase type 1: Purification from human liver and characterization as carbonyl reductase of xenobiotics. *Mol Cell Endocrinol* 248:34–37.
3. Elleby B, et al. (2004) High-level production and optimization of monodispersity of 11beta-hydroxysteroid dehydrogenase type 1. *Biochim Biophys Acta* 1700:199–207.
4. Ogg D, et al. (2005) The crystal structure of guinea pig 11beta-hydroxysteroid dehydrogenase type 1 provides a model for enzyme–lipid bilayer interactions. *J Biol Chem* 280:3789–3794.
5. Zhang J, et al. (2005) Crystal structure of murine 11 beta-hydroxysteroid dehydrogenase 1: An important therapeutic target for diabetes. *Biochemistry* 44: 6948–6957.
6. Hosfield DJ, et al. (2005) Conformational flexibility in crystal structures of human 11beta-hydroxysteroid dehydrogenase type I provide insights into glucocorticoid interconversion and enzyme regulation. *J Biol Chem* 280:4639–4648.
7. Mziaut H, Korza G, Hand AR, Gerard C, Ozols J (1999) Targeting proteins to the lumen of endoplasmic reticulum using N-terminal domains of 11beta-hydroxysteroid dehydrogenase and the 50-kDa esterase. *J Biol Chem* 274:14122–14129.
8. Odermatt A, Arnold P, Stauffer A, Frey BM, Frey FJ (1999) The N-terminal anchor sequences of 11beta-hydroxysteroid dehydrogenases determine their orientation in the endoplasmic reticulum membrane. *J Biol Chem* 274:28762–28770.
9. Lavery GG, et al. (2006) Hexose-6-phosphate dehydrogenase knock-out mice lack 11 beta-hydroxysteroid dehydrogenase type 1–mediated glucocorticoid generation. *J Biol Chem* 281:6546–6551.
10. White PC, Rogoff D, McMillan DR, Lavery GG (2007) Hexose 6-phosphate dehydrogenase (H6PD) and corticosteroid metabolism. *Mol Cell Endocrinol* 265-266: 89–92.
11. Bujalska IJ, et al. (2005) Hexose-6-phosphate dehydrogenase confers oxo-reductase activity upon 11β-hydroxysteroid dehydrogenase type 1. *J Mol Endocrinol* 34:675–684.
12. Kotelevtsev Y, et al. (1997) 11beta-hydroxysteroid dehydrogenase type 1 knockout mice show attenuated glucocorticoid-inducible responses and resist hyperglycemia on obesity or stress. *Proc Natl Acad Sci USA* 94:14924–14929.
13. Bujalska IJ, Kumar S, Stewart PM (1997) Does central obesity reflect "Cushing's disease of the omentum"? *Lancet* 349:1210–1213.
14. Taylor NF, Bartlett WA, Dawson DJ (1984) Cortisone reductase deficiency: Evidence for a new inborn error in metabolism of adrenal steroids. *J Endocrinol* 1025:1.
15. Savage MW (1991) Increased metabolic clearance of cortisol in corticosteroid 11-reductase deficiency. *J Endocrinol* 129S:1.
16. Nikkilä H, et al. (1993) Defects in the HSD11 gene encoding 11 beta-hydroxysteroid dehydrogenase are not found in patients with apparent mineralocorticoid excess or 11-oxoreductase deficiency. *J Clin Endocrinol Metab* 77:687–691.
17. Phillipov G, Palermo M, Shackleton CH (1996) Apparent cortisone reductase deficiency: A unique form of hypercortisolism. *J Clin Endocrinol Metab* 81:3855–3860.
18. Jamieson A, et al. (1999) Apparent cortisone reductase deficiency: A functional defect in 11beta-hydroxysteroid dehydrogenase type 1. *J Clin Endocrinol Metab* 84: 3570–3574.
19. Nordenström A, Marcus C, Axelson M, Wedell A, Ritzén EM (1999) Failure of cortisone acetate treatment in congenital adrenal hyperplasia because of defective 11beta-hydroxysteroid dehydrogenase reductase activity. *J Clin Endocrinol Metab* 84: 1210–1213.
20. Lavery GG, et al. (2008) Steroid biomarkers and genetic studies reveal inactivating mutations in hexose-6-phosphate dehydrogenase in patients with cortisone reductase deficiency. *J Clin Endocrinol Metab* 93:3827–3832.
21. Esteban NV, et al. (1991) Daily cortisol production rate in man determined by stable isotope dilution/mass spectrometry. *J Clin Endocrinol Metab* 72:39–45.
22. Lawson AJ, et al. (2009) Mutations of key hydrophobic surface residues of 11 beta-hydroxysteroid dehydrogenase type 1 increase solubility and monodispersity in a bacterial expression system. *Protein Sci* 18:1552–1563.
23. Walker EA, Clark AM, Hewison M, Ride JP, Stewart PM (2001) Functional expression, characterization, and purification of the catalytic domain of human 11-beta-hydroxysteroid dehydrogenase type 1. *J Biol Chem* 276:21343–21350.
24. Filling C, et al. (2002) Critical residues for structure and catalysis in short-chain dehydrogenases/reductases. *J Biol Chem* 277:25677–25684.
25. Obeid J, White PC (1992) Tyr-179 and Lys-183 are essential for enzymatic activity of 11 beta-hydroxysteroid dehydrogenase. *Biochem Biophys Res Commun* 188:222–227.
26. Vijayakumar M, Zhou HX (2001) Salt bridges stabilize the folded structure of barnase. *J Phys Chem B* 105:7334–7340.
27. Strickler SS, et al. (2006) Protein stability and surface electrostatics: A charged relationship. *Biochemistry* 45:2761–2766.
28. Kumar S, Nussinov R (2002) Close-range electrostatic interactions in proteins. *ChemBioChem* 3:604–617.
29. Musafia B, Buchner V, Arad D (1995) Complex salt bridges in proteins: Statistical analysis of structure and function. *J Mol Biol* 254:761–770.
30. Vijayakumar M, et al. (1998) Electrostatic enhancement of diffusion-controlled protein–protein association: Comparison of theory and experiment on barnase and barstar. *J Mol Biol* 278:1015–1024.
31. Gabdoulline RR, Wade RC (2001) Protein–protein association: Investigation of factors influencing association rates by Brownian dynamics simulations. *J Mol Biol* 306: 1139–1155.
32. Hwang CC, Hsu CN, Huang TJ, Chiou SJ, Hong YR (2009) Interactions across the interface contribute the stability of homodimeric 3alpha-hydroxysteroid dehydrogenase/carbonyl reductase. *Arch Biochem Biophys* 490:36–41.
33. Tomlinson JW, Stewart PM (2005) Mechanisms of disease: Selective inhibition of 11beta-hydroxysteroid dehydrogenase type 1 as a novel treatment for the metabolic syndrome. *Nat Clin Pract Endocrinol Metab* 1:92–99.
34. Shackleton CHL (1993) Mass spectrometry in the diagnosis of steroid-related disorders and in hypertension research. *J Steroid Biochem Mol Biol* 45:127–140.
35. Folch B, Rooman M, Dehouck Y (2008) Thermostability of salt bridges versus hydrophobic interactions in proteins probed by statistical potentials. *J Chem Inf Model* 48:119–127.
36. Pettersen EF, et al. (2004) UCSF Chimera—a visualization system for exploratory research and analysis. *J Comput Chem* 25:1605–1612.